

Deformation behavior of Cu-composites processed by HPT

L Krämer¹, S Wurster² and R Pippan¹

¹Erich Schmid Institute of Materials Science, Austrian Academy of Sciences, Austria

²Department of Materials Physics, University of Leoben, Austria

E-mail: lisa.kraemer@stud.unileoben.ac.at

Abstract. Deformation behavior of two phase materials with High-Pressure Torsion (HPT) was investigated on the basis of Cu-composites. As second phases Fe, W and yttria were used. The deformation behavior in the HPT-process differs due to their different mechanical properties and the ratio of Cu and the second phase. A large benefit of deforming two-phase materials is the homogenous nanocrystalline microstructure with smaller achievable grain sizes than in single phase materials subjected to HPT. Attention is given to development of hardness as a function of the applied strain, the chemical composition at different radii and the obtained microstructure. Tensile tests provide additional information about strength.

1. Introduction

HPT-deformed, single phase materials show a larger saturation grain size than two phase materials. Pure Cu shows after Severe Plastic Deformation (SPD) different saturation grain sizes depending on the purity of the used Cu (80 nm to 90 nm [1], 200 nm [2], 250 nm [3], 300 nm [4]). Different two phase materials were deformed by HPT to achieve a smaller saturation grain size and so a finer microstructure. To compare the influence of the second phase in this study, a softer and a harder bcc-material (Fe and W, respectively) and a brittle ceramic phase (Y_2O_3) were mixed with Cu.

In contrary to single phase deformation, it has been shown for W-Cu bulk materials that after an equivalent strain of $\epsilon_v = 256$ at room temperature the particle size of W is 10 nm to 20 nm and it does not change after applying more strain [5–7]. Until then, the fragmentation of W-particles follows a fractal distribution [6]. The refinement of the harder W in the softer Cu can be explained by a localized region with high plastic deformation where also the W-particles are deformed until the plastic deformation spreads throughout the whole sample because of the strong strain-hardening in the localized region [8].

In recent years, it was tried for Cu-Fe to generate a supersaturated solid solution using the HPT-process. As soon as the Fe- or Cu-fragments go below a certain size, they become unstable because of capillary pressure [9]. During heating, the supersaturated solid solution becomes unstable and pure nm-scaled Cu- and Fe-crystals begin to evolve. This can be used to produce nanocrystalline materials with a grain size of about 15 nm being smaller than the grain size achievable with HPT deformation of the pure materials (300 nm for Cu and 400 nm for Fe). The obtained structures are stable up to annealing temperatures of 620 °C for 1 h before grain growth occurs. Interesting is the fact that the hardness of the supersaturated solid solution increases with increasing annealing temperature until the material decomposes and the hardness decreases [4].

Stobrawa et al. [10] produced Cu-yttria microcomposites with different compositions by milling Cu and Y_2O_3 powders in a planetary ball mill in an argon-methanol atmosphere for 30 h. This was done until the particle size was below 200 nm with a majority share of 20 nm to 40 nm particles. After milling, low temperature sintering at 550 °C to 570 °C was conducted. The grain



size did not increase during sintering, but the danger of agglomeration of the nanocrystalline powder or increasing porosity of the sintered material exists. The compression tests show that a higher amount of Y_2O_3 increases the yield strength and up to 1 wt% the plasticity of the material is not reduced. However, samples containing more than 2 wt% Y_2O_3 are brittle.

2. Experimental

As initial material for the majority of the produced specimen, powders were used. Additionally, two bulk materials produced by Plansee SE, Austria (W - 10 wt% Cu and W - 25 wt% Cu) and one pure Cu-bulk material (Cu: 99,9% purity) were used as reference materials. Comparison of results from HPT-specimens produced via the powder route or from bulk materials allows to study the influence of the powder route on the microstructure and the mechanical properties of the final bulk material. Due to the large specific surface of powders and the decrease of purity, the properties of the produced materials might be changed in comparison to initial bulk specimens. Powders were measured (Cu - 25 wt% W, Cu - 12 wt% Fe - equals the vol% of W - and Cu - 4 wt% Y_2O_3) and mixed. Two different HPT-devices were used in a two-step process. First, larger samples were produced with an HPT-device with a maximal force of 4000 kN, but due to the used high force and amount of material, the deformation causes heating of the material. To minimize this effect, only a low deformation velocity (≈ 0.07 rpm) can be used. The second HPT-device can deform smaller specimen with a maximal force of 400 kN and a velocity of ≈ 0.7 rpm. One big advantage of the smaller HPT-engine is the possibility of deforming not only at room temperature, but in a temperature range from -196 °C to 720 °C.

After mixing the powders, they are filled into a Cu-ring with an outer diameter being larger than the cavity of the anvils. The ring is glued on the lower anvil of the larger HPT-device. The inner diameter of the Cu-ring is as large as the cavity and thereby the amount of material that can be processed, is maximized. The anvils are closed, force of approximately 210 kN is applied and one anvil is rotated for 2° to 3° against the other. The compact disc has to be removed so that the flattened Cu-ring can be cut off. That is important in order to prevent cracks from growing from the edge to the center on the one hand and on the other, to prohibit the mixing of Cu of the ring with the powder and thereby, changing the percentages of Cu in the specimen.

The disc is placed again in the anvil and is deformed for 10 turns at room temperature. The final dimensions of the HPT-samples are 4 cm in diameter and 7 mm in height. Afterward, it is cut into half with a cutting disc (Struers Secotom) and a slice with a thickness of 2 mm is produced that can be used for hardness measurement. For the second HPT-step, two pieces (8 mm thick) are cut parallel to the first cuts and are turned round to a cylinder with a diameter of 7 mm to 8 mm. These two cylinders are not fully circular as the height of the first large HPT-disc is smaller than the radius of the cylinders, but due to the compression deformation in the second HPT-step this is compensated. For the second HPT-step, pieces are cut off the cylinders at different radii (0 mm to 8.5 mm) which are approximately 0.8 mm thick.

The microstructure was characterized in a scanning electron microscope (SEM) type LEO 1525 using secondary electrons (SE) or backscattered electrons (BSE). For determination of the chemical composition of the produced materials, energy dispersive X-ray analyzes (EDX) were performed at the SEM LEO 1525. Typical settings used were a voltage of 15 kV to 20 kV and a working distance between 0.5 cm and 1 cm, but for EDX scans larger distances were used. Contrast and brightness of SEM micrographs were adjusted to improve the distinguishability.

The grain size of Cu in selected materials was determined with linear intercept method by using SEM-micrographs. Six lines (two in shear direction, two perpendicular to the shear direction and two under 45°) were used.

To characterize the particle size of W, SEM-images were used. For the evaluation with ImageJ,

ellipsoidal particles were assumed.

The Vickers hardness was measured with BUEHLER Microsмет using 500 g or 1000 g along the radii of the specimen divided in half. Hence, the correlation between hardness and strain can be seen. The distance between the measured points was 250 μm for small indentations and 500 μm for larger ones.

Tensile tests were conducted at room temperature to determine mechanical properties in dependence of the resulting microstructure as a function of the chemical composition and the applied strain. After the second HPT-step, the sample thickness is only about 450 μm which complicates testing as the maximal diameter of the tensile specimen must be smaller. The average diameter was about 300 μm and even so not all samples could be produced fully circular, nevertheless, the correct cross-section area was taken into account for evaluation of stress. The HPT-discs were cut into halves after the second HPT-step, so that material at the edge (at radius 1.5 mm to 2 mm), which has experienced more strain, could be tested. The distance between shoulders was 3.7 mm.

To reduce geometrical mistakes as shoulder offset and the thermal influence during specimen production, the circular grinding tool developed by G. Rathmayr was used [11]. This tool consists of a grinding disc, an adjustable specimen holder, a liquid cooling system and a dial gauge. There are two shafts with a fixation for the samples in the specimen holder, which are synchronically driven by a motor. Due to this fact, the twisting moment on the sample is almost zero, because no side can slow down or accelerate individually. To measure the position of the specimen holder on the linear bearing, a dial gauge is used. The linear bearing is perpendicular to the axes of the grinding disc, so that the rotation axis of the specimen is perpendicular to the shoulder. For the liquid cooling system, water with some additive (Corrozip from Struers) is used.

As the specimen and the grinding disc rotate, the diameter is adjusted by moving the specimen holder along the linear bearing. After the grinding, an additional polishing step can be conducted. This was omitted because of the danger of breaking the very thin specimens (diameter $\sim 300 \mu\text{m}$). Before testing, the diameter was measured with transmitted light on an optical microscope and it was controlled if the samples were completely circular.

The testing was performed at a Kammrath&Weiss (K&W) miniature tensile testing device and the exact procedure for tensile testing and evaluation is described by Rathmayr et al. [11]. A diode provided the light from underneath the specimen, so that the recorded pictures show a high contrast between the sample (dark) and the background (light).

The specimens were lying on the holder to avoid bending and only plasticine was used to absorb the released energy upon fracture and prevent the specimen from flying away. The speed of testing was $2.5 \mu\text{m s}^{-1}$. During testing, pictures of the sample were taken with a single lens flex camera. They are used to determine the changing specimen geometry such as the thickness reduction and the increase in length. With this information available, it is possible to calculate stress-strain values by using a Matlab package written by G. Rathmayr [11].

3. Results and Discussion

3.1. Hardness and microstructure investigation

In Figure 1, it can be observed that Cu - 25 wt% W, Cu - 4 wt% Y_2O_3 and Cu-powder obtain the same value of hardness after a low amount of applied strain, while the hardness of Cu - 12 wt% Fe is higher and the hardness of Cu-bulk is lower. The differences between Fe and W or Y_2O_3 result from the different hardness of single phase materials and the miscibility due to different crystal structure and atomic bonding. On the one hand, the hardness of Fe is similar to Cu and therefore, it is easier to co-deform both phases by HPT, on the other hand, W and

Y_2O_3 are nearly immiscible. These facts lead to a finer microstructure (Table 1) and so, to the higher hardness of Cu - 12 wt% Fe after only a low amount of strain. The lower hardness of HPT-deformed Cu-bulk can be explained by the higher purity of the bulk material compared to the HPT-deformed Cu-powder. The large surface of powder and the contact with the environment leads to an increase of impurities which cannot be detected by standard EDX. However, the microstructure of HPT-deformed Cu-powder is finer than of HPT-deformed Cu-bulk, because impurities stabilize the grains and slow down grain growth (Table 1).

Finally, it can be concluded that after an equivalent strain of $\epsilon_v = 1000$, hard second phases as yttria and W do not contribute strongly to the hardness, but impurities in the Cu matrix sustain a major part. Only at higher strains, W and Y_2O_3 increase the hardness further up to nearly 300 HV and a saturation cannot be found even at an equivalent strain of $\epsilon_v = 10000$. The decrease and later increase of hardness of Cu - 12 wt% Fe samples deformed for 200 and 400 turns cannot be explained in detail. One idea is that the material becomes a supersaturated solid solution and due to the heat of deformation and friction during additional turns the HPT-disc is heated up and so coarsening or segregation takes place. This might explain the decrease of hardness after 200 turns and the increase of hardness after 400 turns due to the formation of a very fine nanoscaled structure (≈ 70 nm).

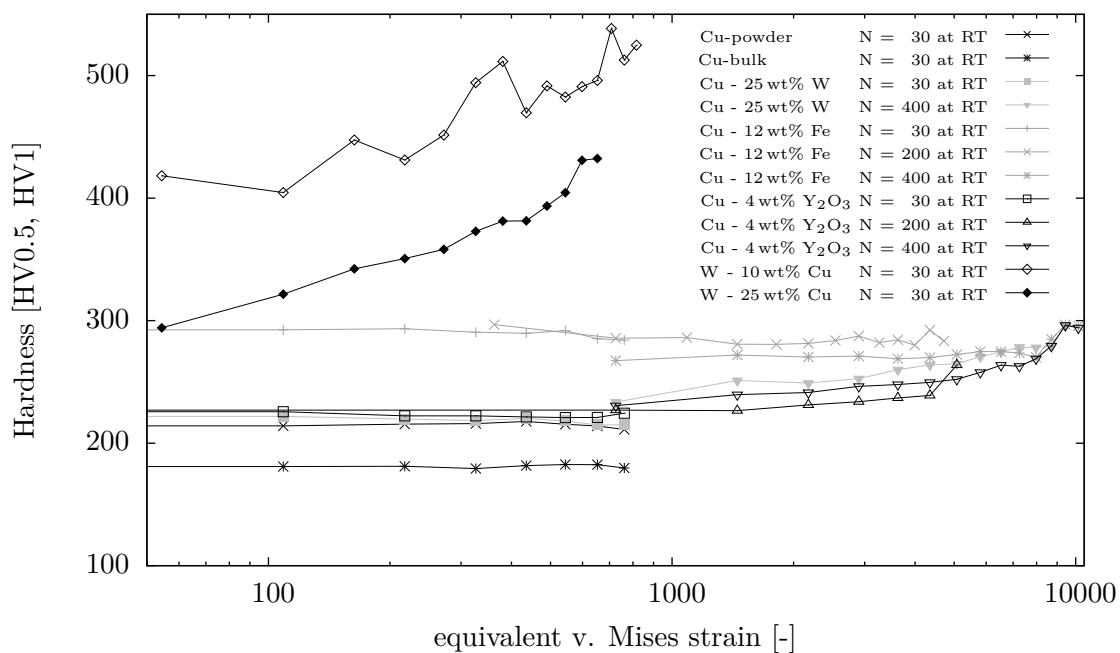


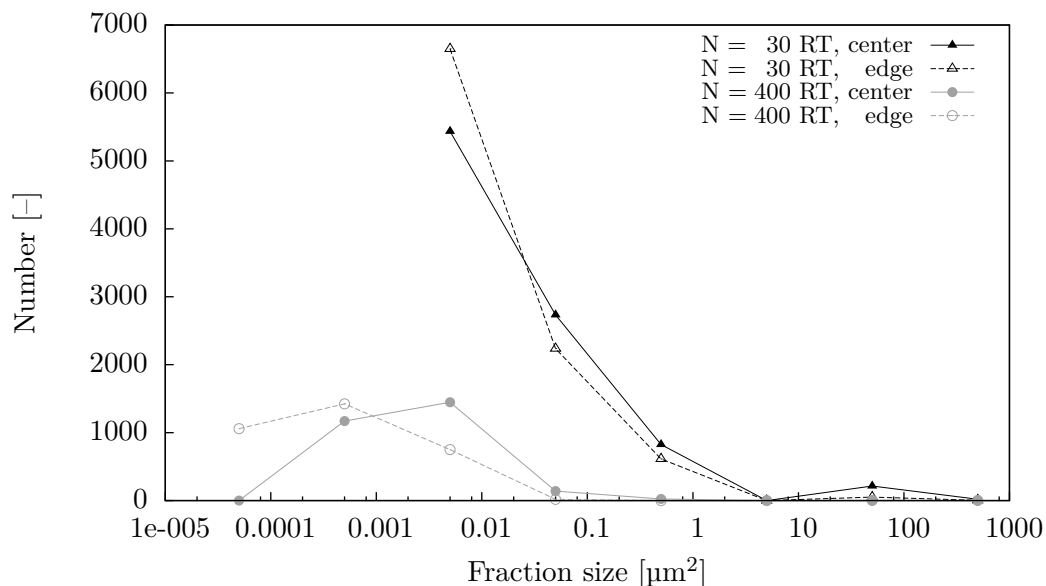
Figure 1: Vickers hardness as function of equivalent v. Mises strain. Notice the logarithmic scale for equivalent strain. The hardness depends on chemical composition: Fe-particles influences it even at low strains, whereas W and yttria only distribute and increase hardness after higher deformations.

It is difficult to deform a small amount of hard particles in a softer matrix because the majority of the strain is only realized by Cu. Although the plastic deformation in Cu is high, a majority of the harder particles just flow in the matrix without changing their form or breaking up. Depending on the strain, the distribution of the particle size shifts at higher radius to smaller values as the number of large particles strongly decreases (Figure 2).

In Figure 3f the Cu-matrix flows around a circular Fe-particle. Figure 3c shows the deformation and flowing behavior of the matrix and small W-particles near a large W-agglomerate: The

Table 1: Grain size of the Cu-matrix after HPT-deformation near the center and the edge

		Number of turns [-]	Grain size near the center [nm]	Grain size near the edge [nm]
1	Cu-powder	30	300	240
2	Cu-bulk	30	520	470
3	Cu - 25 wt% W	30	250	120
4	Cu - 25 wt% W	400	120	100
5	Cu - 12 wt% Fe	30	120	100
6	Cu - 12 wt% Fe	400	100	<70
7	Cu - 4 wt% Y ₂ O ₃	30	230	150

**Figure 2:** Fraction size distribution of W-particles after 30 and 400 turns near the center and the edge. The low number after 400 turns is due to the limited SEM resolution.

small dispersoids in the range of 50 nm to 100 nm become more elongated and align in the direction of the flow. Near the large agglomerate the particles are parallel to the shear direction. To obtain such a distribution, the strain along the large particle must be higher than in the remaining matrix. This is very similar to phenomenon in fluid mechanics where the velocity of a fluid that flows around an obstacle is higher. Yttria is more brittle than W and cannot be deformed in Cu even at high strains. So, in Figure 3 the form of the Y₂O₃-particles does not change and only the size becomes smaller as the breaking down of particles increases with the applied strains (compare near center (g) and edge (h) of the HPT-disc). In contrary, Fe and Cu are similarly deformable, which has a big impact on the way of deformation. Not only the Cu-grains refine quickly, but also the Fe-particles break down. Compared to the center of a Cu- 12 wt% Fe sample (Figure 3d) the fraction of larger Fe-particles nearly vanishes at the edge (Figure 3e).

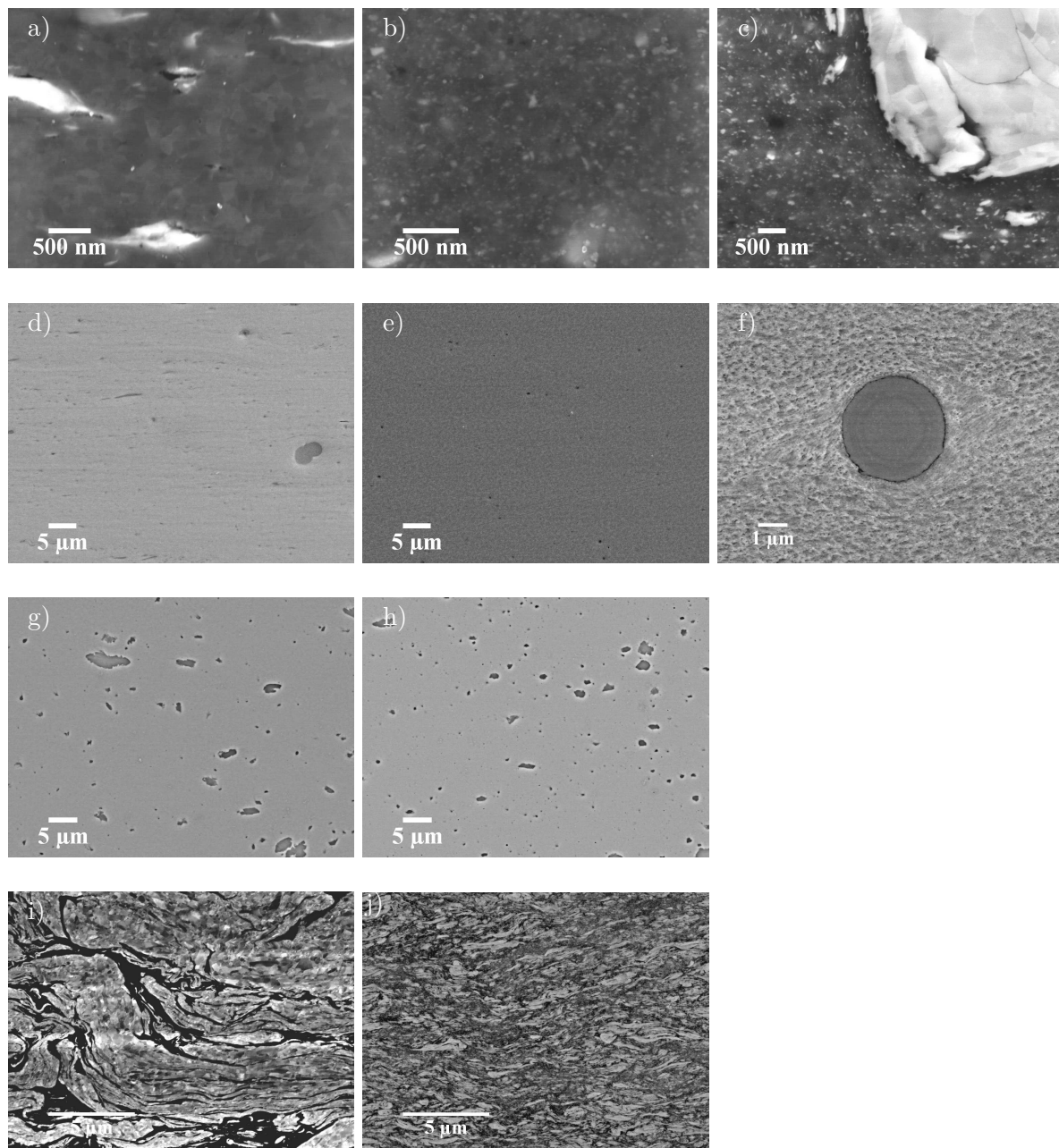


Figure 3: SEM-micrographs of specimens after 30 turns at room temperature. (a-c) Cu - 25 wt% W: The grain size of Cu refines with higher strain, i.e. from near the center (a) to the edge of the specimen (b). In (c) Cu-matrix with small W-particle flow around a large W-agglomerate. (d-f) Cu - 12 wt% Fe: The size of Fe-particles decreases from the center (d) to the edge (e) of the specimen, eg. at higher strains. In (f) the flow of the Cu-matrix around an almost perfectly circular Fe-particle can be seen. (g,h) Cu - 4 wt% yttria: The yttria-particles do not change their shape between center (g) and edge (h), but with higher strain their size decreases due to fracturing of particles and clusters of particles. SEM-micrographs (BSE) near the edge of W - 10 wt% Cu (i) and W - 25 wt% Cu (j) after 30 turns at room temperature: The microstructure refines stronger for W - 25 wt% Cu.

3.2. Influence of particle morphology and volume percentage of the second phase

The refinement of the second phase depends to some extent also on its morphology. Circular particles (Figure 3f) and agglomerates of small, strong powder particles are very stable and high applied strain is needed for deformation or breaking. However, if the applied strain is high enough, even the most stable particles refine and reinforce the Cu-matrix. Thus, the morphology does not have an impact on the results at very high strains where saturation is reached, but on the amount of strain that is needed to reach this saturation.

Not only the mechanical properties and morphology influence the deformation behavior, but also the ratio of volume of the harder to the softer phase. If the volume of the softer phase is significantly larger, the majority of plastic deformation can take place there. However, as soon as the volume of the harder phase reaches the extent of the matrix, the strain in the harder phase increases too (compare Figure 3i to Figure 3j). This can be demonstrated using the industrially produced bulk materials containing 10 wt% (\approx 20 vol%) Cu and 25 wt% (\approx 40 vol%) Cu. A higher amount of W has two consequences: Larger areas of W are teared apart and the grain size of Cu as well as of W decreases strongly. If samples with drastically different percentages of W are compared (Figure 3a,b to 3i,j), W - 25 wt% Cu shows the most homogenous microstructure. To obtain uniform microstructure after a strain as small as possible, the volumes of the soft and hard phase should be equal (25 wt% Cu equals approximately 40 vol% Cu). If enough strain is applied the out-coming microstructure does not depend on the starting microstructure. However, by using a finer initial composite homogeneity only will be reached sooner.

Sabirov et al. [8] also deformed W - 25 wt% Cu produced by Plansee SE, Austria but the initial particle size of W was 2 μ m. Whereas in this work, it was between 5 μ m to 10 μ m. The coarser initial material showed after 100 turns the same fine homogenous microstructure as it was achieved by Sabirov et al. after 30 turns. Hence, if the applied strain is high enough the ratio between soft and hard phase does not matter and the particles break up.

3.3. Mechanical characterization

Tensile testing shows one of the most important drawbacks of using powder as initial material. Because of impurities, the fracture strength is higher and fracture strain is lower compared to bulk material with the same composition (compare Figure 4, Cu-powder and Cu-bulk). Fe strongly improves the properties of powder-processed samples as it increases not only strength but also encourages strain hardening. By comparison of SEM-micrographs, it can be concluded that this is obtained not only because of the ductile behavior of Fe-dispersoids but also due to their fine distribution (Figure 5b).

Y₂O₃- (Figure 5c) and W-agglomerates (Figure 5a) are larger than Fe-particles and some agglomerates can always be found on the fracture surface. This explains also why W-reinforced Cu shows inferior results in tensile testing compared to yttria-reinforced Cu: In the tested samples the volume fraction of W is higher than that of yttria and so the proportion of large W-particles and agglomerates is also larger. Thus, it is more likely to find one large, defect-containing agglomerate within the gauge length. This will promote fracture. The importance of the fraction of the brittle phase can be also observed in the two samples produced from the Plansee materials: The sample with the highest amount of Cu not only shows the highest fracture strength, but also the highest fracture strain. Additional SEM-micrographs show that the microstructure refines better with higher amount of Cu (Figure 3i and 3j) and also the fracture surface becomes more smooth (Figure 5f and 5e) [12].

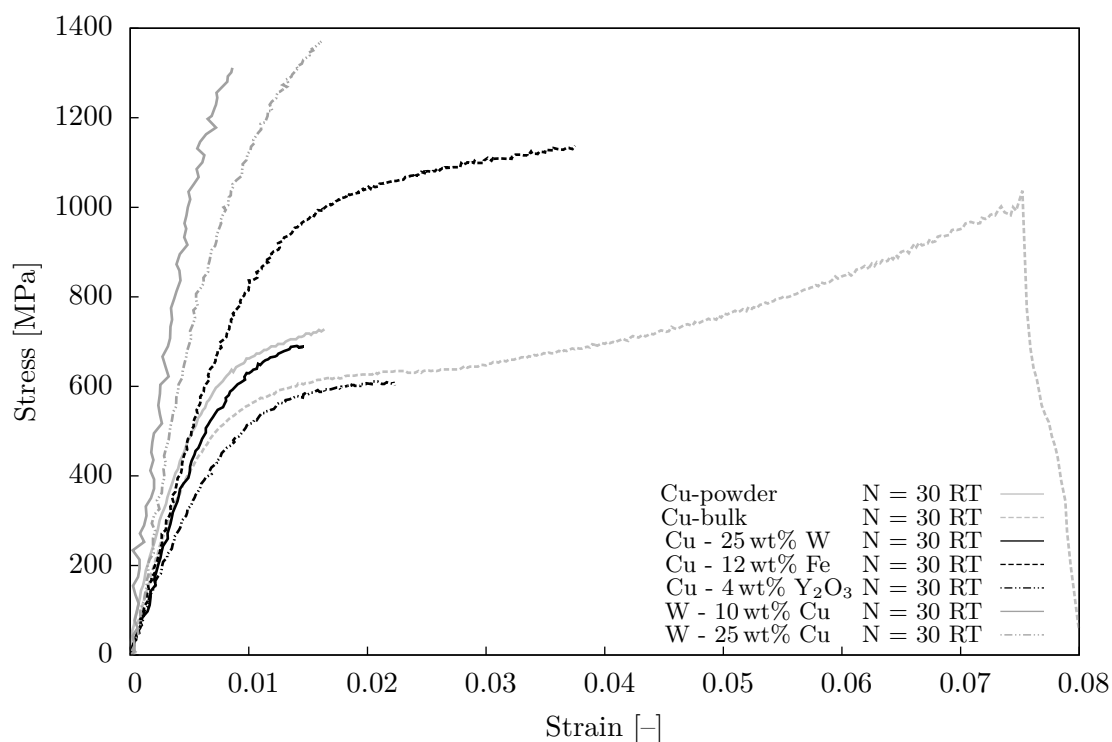


Figure 4: Comparison of tensile test data of the investigated materials after a HPT-deformation for 30 turns at room temperature. Interesting is that reinforcing with W and yttria hardly influences the behavior of Cu-powder, but Fe does.

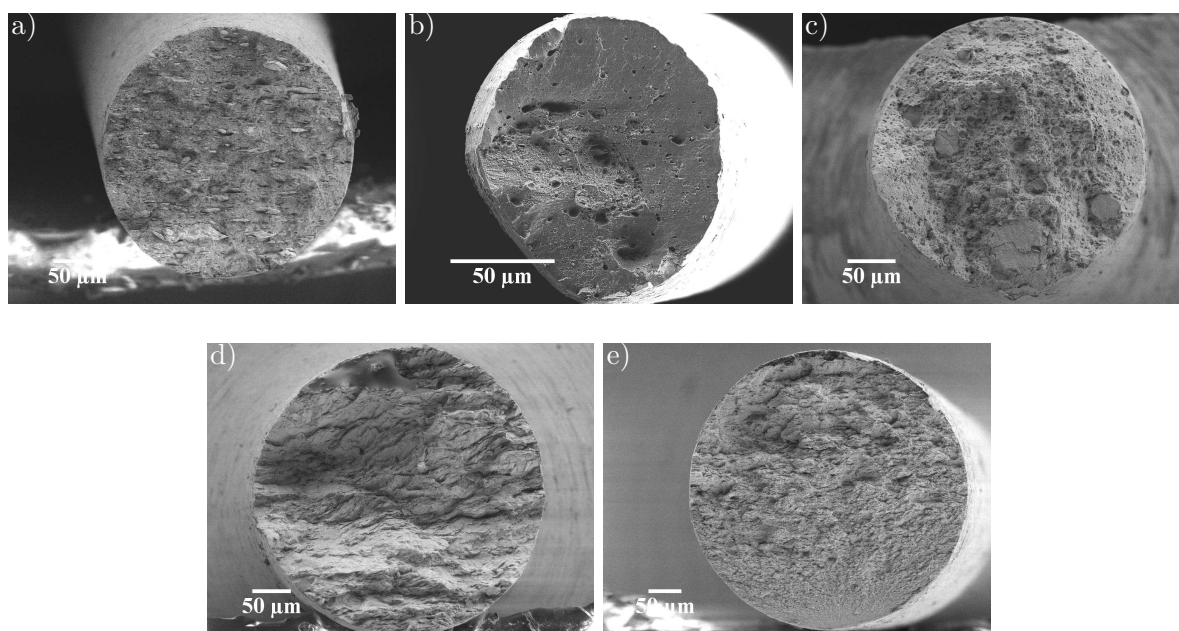


Figure 5: SEM-fractographs of tensile samples: (a)Cu - 25 wt% W, (b)Cu - 12 wt% Fe, (c)Cu - 4 wt% Y₂O₃, (d)W - 10 wt% Cu, (e)W - 25 wt% Cu. All samples were deformed for 30 turns at room temperature.

4. Conclusion

Out of the used materials, Cu - Fe was the easiest to deform and a homogenous structure was soon reached with improved hardness as well as good tensile strength. This could be explained by the similar hardness of Cu and Fe which enables a simultaneous deformation of both phases and promotes the development of a very fine microstructure. The deformability is also increased by the little, but nevertheless existing, mutual solubility which enables to produce a supersaturated solid solution. The ceramic phase Y_2O_3 shows brittle behavior and particles are not deformed plastically before breaking. Therefore, the fracture strain is very little in tensile testing. For W the deformability as well as solubility are smaller than for Fe and the same homogeneous microstructure cannot be reached. Only after application of significant higher strain, the hardness approaches the same values as for Cu - Fe. If the portion of W is increased the material is forced to deform simultaneously and the best results regarding fast co-deformation are obtained with specimens containing a similar volume of the hard and the soft phase (W - 25 wt% Cu).

Disclaimer

This work, supported by the European Commission under the Contract of Association between EUROTOM and the Austrian Academy of Sciences, was carried out within the framework of the European Fusion Development Agreement. The views and opinions expressed herein do not necessarily reflect those of the European Commission.

5. References

- [1] Valiev, R. Z., Islamgaliev, R. K., and Alexandrov, I. V. (2000) *Progress in Materials Science* **2**, 103–189.
- [2] Mishra, A., Kad, B. K., Gregori, F., and Meyers, M. A. (2007) *Acta Materialia* **55**, 13–28.
- [3] Schafner, E. and Kerber, M. (2007) *Materials Science and Engineering A: Structural Materials: Properties, Microstructures and Processing* **462(1-2)**, 139–143.
- [4] Bachmaier, A. Generation of bulk nanocomposites by severe plastic deformation PhD thesis University of Leoben (2011).
- [5] Edwards, D., Sabirov, I., Sigle, W., and Pippan, R. (2012) *Philosophical Magazine* **92(33)**, 4151–4166.
- [6] Sabirov, I. and Pippan, R. (2007) *Materials Characterization* **58(10)**, 848–853.
- [7] Schöberl, T., Sabirov, I., and Pippan, R. (2005) *Z. Metallkd.* **96**, 1056–1062.
- [8] Sabirov, I. and Pippan, R. (2005) *Scripta Materialia* **52(12)**, 1293–1298.
- [9] Sauvage, X., Wetscher, F., and Pareige, P. (2005) *Acta Materialia* **53**, 2127–2135.
- [10] Stobrawa, J., Rdzawski, Z., and Gluchowski, W. (2007) *Journal of Achievements in Materials and Manufacturing Engineering* **24(2)**, 83–86.
- [11] Rathmayr, G., Bachmaier, A., and Pippan, R. (2013) *Journal of Testing and Evaluation* **41(4)**, 635–646.
- [12] Krämer, L. Production and characterization of particle-stabilized nanocrystalline Cu for high temperature applications Master's thesis University of Leoben (2014).